Available online at www.sciencedirect.com

ScienceDirect

journal homepage: www.elsevier.com/locate/issn/15375110

Research Paper

Performance comparison of charging systems for autonomous electric field tractors using dynamic simulation

Oscar Lagnelöv[*], *Gunnar Larsson*, *Daniel Nilsson*, *Anders Larsolle*, *Per-Anders Hansson*

Swedish University of Agricultural Sciences, Department of Energy and Technology, P.O Box 7032, SE-75007, Sweden

ARTICLE INFO

Article history:
Received 4 November 2019
Received in revised form
12 March 2020
Accepted 19 March 2020
Published online 14 April 2020

Keywords:
Tractor
BEV
Modelling
Simulation
Conductive Charging
Battery Exchange

A model simulating an autonomous battery electric vehicle system for agricultural field use was created, assuming a 200-ha conventional cereal farm in Swedish conditions. The different subsystems were verified against sources in the literature, field experiments and general common practice. The model was used to compare two different charging systems (conductive charging and battery exchange) for battery electric tractors to each other. A comparative simulation was made with conventional diesel systems (fully autonomous or manned for 10 h d^{-1}). The simulation results indicated that battery exchange was generally a faster system than conductive charging. The results also showed that both electric systems were able to achieve similar active time during spring field operations as a corresponding system of a simulated manned diesel tractor for battery sizes from 50 kWh and charge powers from 50 kW.

1. Introduction

Agricultural field machinery is currently almost exclusively driven by internal combustion engines (ICEs), usually diesels. There are various research paths as regarding renewable drive options, with electric drive seen as a natural step in the evolution of heavy vehicles (Andersson, 2019; Moreda, Muñoz-García, & Barreiro, 2016). In recent years, there have been significant developments in off-road electric drives for mining loaders, excavators, heavy-duty dump trucks and also agricultural vehicles (Moreda et al., 2016).

Battery electric vehicles (BEV) for agricultural field work have been described previously (Alcock, 1983; Engström & Lagnelöv, 2018; Moreda et al., 2016; Volpato, Paula, Barbosa, & Volpato, 2016, p. 162458121), but have not made significant inroads on the market. Previous studies have indicated that conventionally sized field-work tractors with a battery electric drives reduce emissions, increase driveline efficiency and

* *Corresponding author.*
E-mail address: oscar.lagnelov@slu.se (O. Lagnelöv).
https://doi.org/10.1016/j.biosystemseng.2020.03.017

Nomenclature

A, B, C	Machine parameters
A	Vehicle front area (m^2)
a	Acceleration ($m\ s^{-2}$)
B_n	Machine/soil ratio parameter
BES	Battery exchange system
BED	Battery electric drive
BEV	Battery electric vehicle
C_D, C_{rr}	Drag and rolling resistance coefficients (decimal)
C_o	Overall rate of work ($ha\ h^{-1}$)
CC	Conductive charging
CC/CV	Constant current/constant voltage
D_F	Distance field-to-farm (km)
D_T	Tillage depth (m)
DES	Discrete Event Simulation
E_R	Rated battery energy content (kW h)
E_B	Battery energy content (kW h)
E_{Road}	Road transport energy requirement (kW h)
FC	Field capacity of soil ($mm\ m^{-1}$)
f_i	Soil texture adjustment parameter
F_{MR}	Motion resistance (kN)
F_{Road}, F_{Field}	Sum of forces on vehicle when on road/field (N)
F_a, F_{grad}, F_{drag}, F_{rr}	Acceleration, gradient, drag and rolling resistance forces (N)
F_N	Normal force (N)
F_D	Draught force (N)
n	Field order number
ICE	Internal combustion engine
m_a	Soil moisture content (mm)
x	Field task
m_p	Soil moisture content at previous time step (mm)
m	Mass (kg)
N_B	Number of additional batteries
N_V	Number of vehicles
N_C	Number of chargers
P_C	Charger power (kW)
P_D	Draft power requirement (kW)
P_{Field}	Total field work power requirement (kW)
P_R	Rated vehicle power (kW)
P_V	Vehicle power (kW)
Q_d	Drainage water flow (mm)
Q_r	Run-off water flow (mm)
Q_e	Evapotranspiration water flow (mm)
S, S_{Road}	Field and road speed ($km\ h^{-1}$)
s	Slippage (decimal)
SoC, θ	State of charge
θ_{min}	Minimum state of charge (decimal)
θ_{max}	Maximum state of charge (decimal)
$\theta(t)$	State of charge at time t (decimal)
t	Simulation time (h)
T_{cc}	Charging time (h)
T_{Field}	Available work time before recharging (h)
T_D	Total active time (d
T_{Spring}	Total active time during spring (d)
v	Vehicle speed ($m\ s^{-1}$)
W	Machine width (m or no. of tools)
X	Fieldwork task
α	Gradient (%)
η_{Field}	Field efficiency factor (decimal)
η_{Motor}, $\eta_{Transmission}$, $\eta_{Battery}$, $\eta_{Charger}$	Efficiency factors (decimal)
ρ_{air}	Density of air ($kg\ m^{-3}$)

lower fuel import dependency (Engström & Lagnelöv, 2018). The benefits are achieved at the expense of lower profitability, since battery electric drives are less compatible with the normal working hours of tractor drivers. This is because the energy storage capacity of batteries is generally too low to support several hours of heavy field work, which would require recharging repeatedly during the working day or choosing a large battery. In a study on a John Deere field tractor, a battery of 130 kWh was not sufficient for an entire working day requiring a 3-h recharge after 4 h of mixed field work (John Deere, 2017). Thus, using a battery electric drive (BED) tractor would lead to a trade-off between a longer working day for the driver or a reduced total field time, so conventional-sized, manned BED tractors are currently not an economically competitive option for field operations.

There are two options to overcome this, autonomous drive and rapid recharging systems. Autonomous drive could enable a similar or higher workload by operating a low-powered vehicle for a larger proportion of the day compared with a conventional, manned tractor. Several autonomous agricultural vehicles currently exist in various stages of development. These range from vehicles based on conventional tractors (Case IH Agriculture, 2019; Oksanen, 2015) to small robots designed for very specific tasks (Fendt, 2017; Young, Kayacan, & Peschel, 2018) and even smaller autonomous implement carriers like Thorvald II (Grimstad & From, 2017), SRFV (Bawden, Ball, Kulk, Perez, & Russell, 2014; Young et al., 2018) and Robotti (AgroIntelli, 2019; Green et al., 2014).

There are currently two main solutions for BEVs to achieve faster, more optimised recharging: conventional plug-in conductive charging (CC) with a high-power contact charger (commonly used with on-road BEVs), or the use of exchangeable battery packs that recharge at lower power. The latter are mainly used in industries where a high vehicle uptime is essential, such as in city-buses or forklifts in depots and warehouses. In a previous study, one such battery exchange system (BES, also called battery-swap system) was shown to replace a city bus battery in 60 s without needing manual assistance (Song & Choi, 2015). Several of the needs match those in agriculture, so the method should theoretically fit in agricultural applications.

The aim of this modelling study was to compare two different battery recharging methods (CC and BES) with regard to active time required, time distribution and energy use for multi-vehicle BED systems. Comparisons with simulated diesel-driven vehicle systems were also made. The model used was a dynamic model designed to simulate a BEV system for agricultural field operations in a Swedish context.

Table 1 – Properties of the model fields. All crops were grown on an equal number of fields. Distances based on the assumption that field work started on fields closest to the farm centre.

Crop	Field size [ha]	Distance field-to-farm [D_F, km]	Field order no. [n]
Barley	22, 13, 15	2, 2, 6	3, 4, 11
Oats	10, 26, 14	1, 3, 4	1, 6, 8
Spring wheat	15, 22, 13	3, 5, 6	5, 9, 12
Winter wheat	16, 6, 28	1, 4, 5	2, 7, 10
Total area ha			
Barley	Oats	Spring Wheat	Winter Wheat
50	50	50	50

2. Method

2.1. Farm and crop system

A hypothetical cereal farm of 200 ha, located in Uppsala, Sweden, and operated during one growing season, was modelled. The cereal farm was assumed to grow barley, oats, winter wheat and spring wheat, in equal amounts (Table 1). Barley, oats and winter wheat are the most commonly grown cereals in Sweden (Statistics Sweden, 2018), while spring wheat is a normal complementary cereal.

The cropping period was split into three working periods, spring, summer and autumn (Fig. 1). The operations in each working period followed a typical conventional cereal-dominated cropping system in Sweden, with soil cultivation and drilling (in autumn or spring), use of mineral fertilisers, spraying with chemical pesticides and combine harvesting. The necessary field operations were decided by the crop grown on each field according to normal agricultural practices. The intervals between the working periods were designated non-active growing periods in which no operations were required.

The number of days assumed for each period was based on data for Swedish wheat fields (Nilsson, 1976) (Table 2). Dates for the working periods for winter wheat and barley were similar to those described by Myrbeck (1998) for the Uppsala region. The start dates shown in Table 2 were used to trigger the start of operations within each period (i.e. spring, summer, autumn) and the non-active growing periods, when no operations were scheduled and the tractors were inactive. If tasks from the previous period were delayed, they were assumed to be completed before the next period began.

2.2. Control logic

A dynamic model was developed using discrete event simulation and state-based logic for decision making. The simulation was performed in MATLAB (R2017b, The MathWorks Inc. (Natick, MA, USA)) and its toolboxes Simulink, StateFlow and SimEvent (versions 9.0). A simplified decision tree for the control logic and the different simulation modules and states is shown in Fig. 2. Sections 2.3-2.7 describe in detail the states and modules, in the order shown in Fig. 2.

The model was run with the list of inputs shown in Table 3. The main variable used to evaluate the results was the total number of active days (T_D), which is the sum of all time spent in the following states: field work, road transport, charging and workability control. It was chosen as it represents a metric of the capacity of the system. In addition, the time when each field operation finished was recorded, as was the amount of time spent in each state and the total energy needed.

2.3. Vehicle model

In discrete event simulation, an agent or entity is required. In the present case, the agent was the electric agricultural field

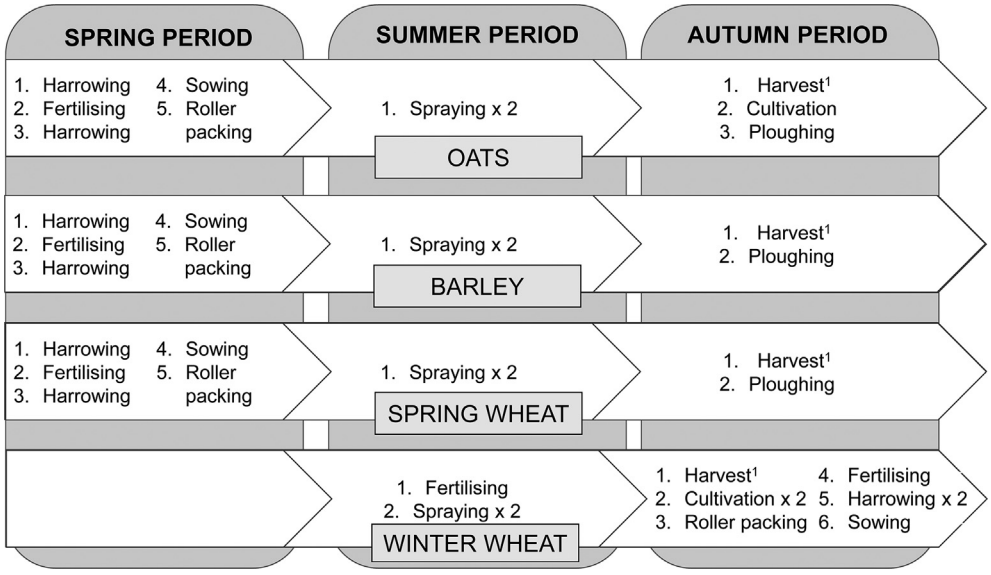

Fig. 1 – Working periods (spring, summer, autumn), crop operations and order of operation in the working periods [1]Harvesting is not included in the simulation, due to use of a combine harvester instead of tractor as the main vehicle.

Table 2 – Definitions of the different working and non-active periods in the model, and the number of days available for each period.

	Start date	No. of days	Simulation time interval [t, h]
Spring period:	16/3	61	0–1464
Non-active period 1	16/5	30	1465–2184
Summer period	15/6	31	2185–2928
Non-active period 2	16/7	47	2929–4056
Autumn period	1/9	61	4057–5520
Simulation end	1/11	–	5520

tractor, modelled as a general BEV. General variables were used for the agent vehicle, instead of empirical technical data, as the aim was to understand the dynamics and the differences between the different charging methods. The main inputs used to define the vehicle were effective vehicle power (P_V) and rated battery energy content (E_R). In addition, rated vehicle power (P_R) denotes the rated engine power for comparison and effective battery energy content (E_B) denotes the useable fractions after losses of E_R:

$$P_V = P_R\ \eta_{Transmission} \quad (1)$$

$$E_B = E_R\ \eta_{Battery}\ (\theta_{max} - \theta_{min}) \quad (2)$$

where, $\eta_{Transmission}$ and $\eta_{Battery}$ are assumed average decimal efficiency factors. Exact values are given in Table A.1 in an appendix to this paper.

Every battery has a dynamic state–of–charge parameter ($\theta(t)$) that varies dynamically between its minimum (θ_{min}) and maximum value (θ_{max}), indicating the fraction of E_R that remains at any given time. It was the only internal battery variable measured for this study.

To better study a multi-vehicle system of smaller vehicles, P_V was kept constant at 50 kW, which gives the vehicles a P_R of 58.5 kW. A permanent magnet direct current motor (Andersson, 2019) was assumed. Different numbers of identical vehicles (N_V) with the qualities P_V and E_R were then created as simulation agents. To study the autonomy of the vehicles, it was assumed that the BED systems worked autonomously for 24 h d^{-1} and the diesel systems had the option of full 24-h autonomy or 10 h of manned operation.

2.4. Soil moisture and workability

Workability is defined by Mueller, Lipiec, Kornecki, and Gebhardt (2011) as the capability of the soil to support tillage. To determine when field operations could be

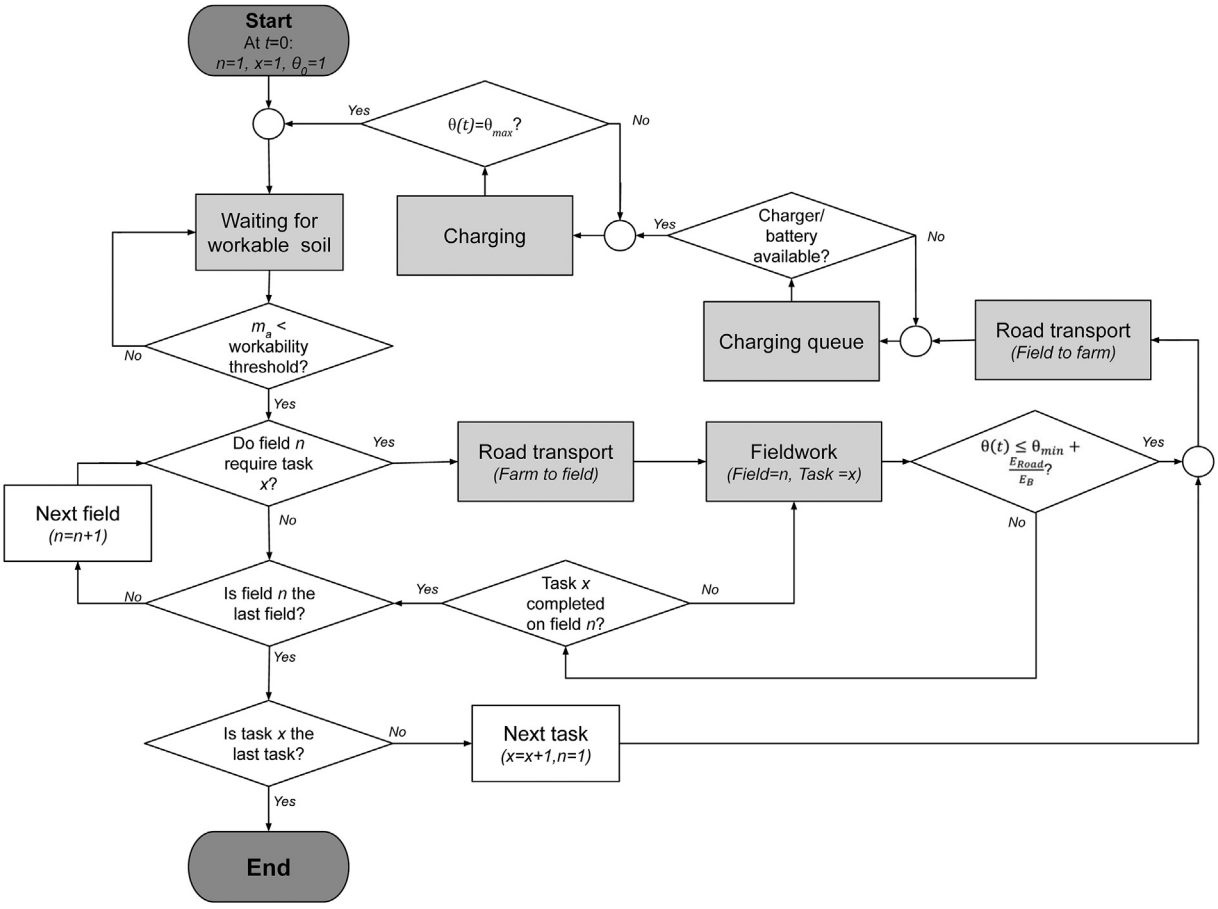

Fig. 2 – Flowchart of the control logic of the vehicle in the simulation. The grey squares represent states and the white diamonds decisions. The dark grey rounded squares represent start and end points, and t, n and x denote time, field number and task number, respectively.

Table 3 – Variable inputs used in the model. Each simulation used a combination of one parameter from each row to define the system configuration. It was assumed that every vehicle had one on-board battery and N_B denotes the number of additional batteries available. For conductive charging (CC), N_B is irrelevant and was not included. The chosen parameters for the base case configurations are shown in bold type.

Input	Range of values
Vehicle power (P_V, kW)	**50**
Charger power (P_C, kW)	10, 25, **50**, 75, 100
Rated battery energy capacity (E_R, kWh)	25, **50**, 75, 100, 150
Yearly weather data	1989–2018
Number of tractors (N_V)	1, **2**, 3, 4, 5
Number of additional batteries (N_B)	**1**, 2, 3,4
Number of chargers (N_C)	**1**, 2, 3

performed, workability based on weather had to be estimated as shown in Fig. 3. The calculated soil moisture level was continuously compared against a threshold for workability taken from de Toro and Hansson (2004). It in turn is based on a value of the field capacity (FC) of clay soils (27.2% or 89.8 mm for a 300 mm soil layer) taken from Witney (1988). A workability threshold of 85% of FC (76.3 mm) was assumed for all general tillage operations except ploughing, for which a threshold of 110% of FC (98.7 mm) was assumed. If the soil moisture content (m_a) was higher than the workability threshold, the vehicle had to wait on the farm until the soil had dried out to below the threshold (Fig. 3). The vehicle then resumed operations. If the vehicle was out in the field, it was assumed to complete its current task before returning to the farm.

In order to calculate soil moisture content, and by extension workability, soil and weather data were needed. The hypothetical Swedish cereal farm was assumed to lie in the production area "Plain districts of Svealand (Ss)" categorised by Myrbeck (1998). The dominant soil type in the region is loamy clay soil with a high clay content (range 25–60%, mainly 40–60%) (Paulsson, Djodjic, Ross, & Hjerpe, 2015). Data on hourly precipitation, monthly mean air temperature and daily number of sunshine hours for the period 1989–2018 were obtained from the Swedish Hydrological and Meteorological Institute (SMHI, 2019). These data derived from different weather stations. A weather station in Uppsala (59.8586, 17.6523) supplied data on precipitation in the periods 1989–2008 and 2013–2018 and on monthly air temperature 1989–2018. As data for some years and some parameters were unavailable from the Uppsala station, other stations nearby were used and similar weather conditions were assumed. A weather station in Enköping (59.6557, 17.1121; 40 km from the Uppsala station) supplied precipitation data for 2009–2012, while a weather station in Stockholm (59.3534, 18.0634; 60 km from the Uppsala station) supplied data on daily number of sunshine hours 2008–2018. Data on number of sunshine hours 1989–2007 were not available from any nearby weather station, so the average value for 2008–2018 was used.

The weather and soil data were used to calculate hourly soil moisture content (m_a) in soils in a temperate climate with the water balance model described by Witney (1988) and Nilsson and Bernesson (2010):

$$m_a = m_p + Q_p - Q_r - Q_d - Q_e \quad (3)$$

where (units mm in all cases): m_p is soil moisture content in the previous time step, Q_p is precipitation, Q_r is surface runoff, Q_d is drainage and Q_e is evapotranspiration, calculated according to Nilsson and Bernesson (2009). This equation is only valid for the top 300 mm of the soil layer and assumes the layer to be uniform.

Values for clay loam and additional values from Witney (1988) were used for Q_p, Q_r, Q_d and Q_e. At the start of the simulation, it was assumed that the soil moisture started at field capacity, due to thawing and early spring precipitation. The validity of the model has been tested by Nilsson and

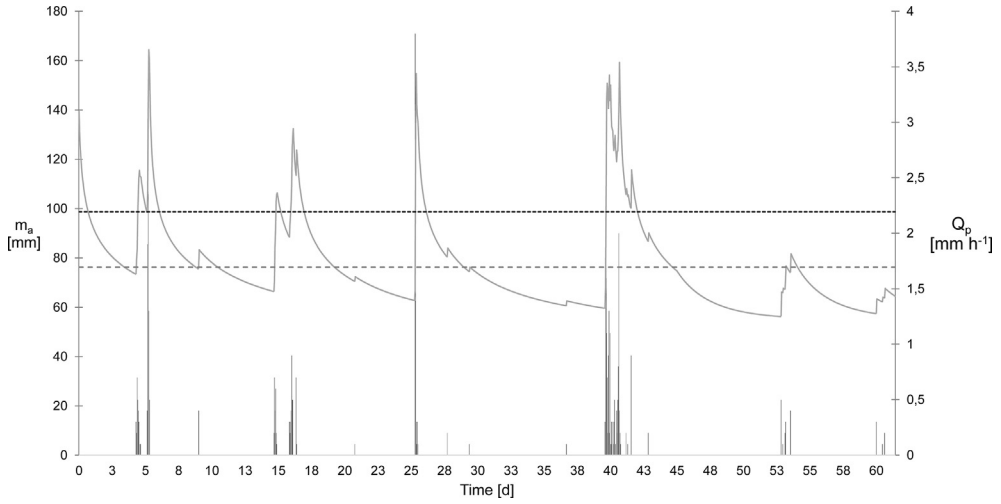

Fig. 3 – Calculated hourly soil moisture content (m_a, solid line) of the top 300 mm soil layer in the spring period (first 61 days of the simulation) using data from 2008. Hourly precipitation (Q_P) is shown as black bars. The workability thresholds for ploughing (black dashed line) and for general tillage (grey dashed line) are also indicated. In 2008, 84% of hours were predicted to be workable for ploughing and 55% for general tillage.

Hansson (2001) against COUP (a hydrological model for soils, previously named SOIL) and found to be adequate.

2.5. Road transport

Each field was assigned a distance from the farm, along with other field parameters (see Table 1). It was assumed that the field operations were executed in order of distance from the farm, starting with the field closest to the farm, represented in the model by the field order number, *n*.

2.5.1. Vehicle dynamics

Calculations of vehicle dynamics were made for the forces acting upon the vehicle on the road (F_{Road}). Rolling resistance, drag force, grading force and acceleration force for road transport were calculated continuously, using equations and constants from Reif and Dietsche (2014):

$$F_{Road} = \Sigma F = F_a + F_{grad} + F_{drag} + F_{rr} \quad (4)$$

$$F_a = m\ a \quad (5)$$

$$F_{grad} = F_N \sin(\alpha) \quad (6)$$

$$F_{drag} = \frac{1}{2}\rho_{air} v^2 C_D A \quad (7)$$

$$F_{rr} = F_N\ C_{rr} \quad (8)$$

where (all in N): F_a is acceleration force, m is vehicle mass in kg, a is acceleration in m s^{-2}, F_{grad} is grading force, F_N is the normal force, α is the gradient or incline angle in degrees (°), F_{drag} is the drag force, ρ_{air} is the density of air in kg m^{-3}, v is the vehicle's speed relative to the air in m s^{-1}, C_D is drag coefficient, A is the frontal area of the vehicle in m^2, F_{rr} is the rolling resistance force and C_{rr} is the rolling resistance coefficient.

The driveline was designed to have peak power and handle accelerations up to 2 m s^{-2} or gradients of up to 10%.

Every road transport event had the following phases: an 1-min acceleration phase where the road speed increased from 0 to 35 km h^{-1} with a maximum acceleration of 2 m s^{-2}, a 1-min deceleration phase where the speed decreased from 35 to 0 km h^{-1} and a remaining time when the vehicle was assumed to travel with an average speed of 35 km h^{-1}, as also assumed in Engström and Lagnelöv (2018) and Engström et al. (2015). The acceleration and deceleration phases included all decelerations and accelerations made during the trip. The resulting total average speed was denoted S_{Road} and expressed in km h^{-1}.

2.6. Fieldwork and operations

The force (F_{Field}) and power (P_{Field}) requirements for field work were based on the vehicle dynamics (Eqs. 4, 5, 6 and 8), with an added factor for the force exerted by the implement (F_D) as shown in Eq. (10). In addition, appropriate values for rolling resistance on clay soil and on-field vehicle speed were used. For exact values, see Table A.1.

The value of F_D was determined for each of the operations in Fig. 1, using empirical implement draft equations and the inherent motion resistance, calculated for firm clay soil based on ASAE (2000):

$$P_{Field}(x) = F_{Field}(x)\ v;\ P_{Field}(x) \leq P_V \quad (9)$$

$$F_{Field}(x) = \Sigma F = F_a + F_{grad} + F_{drag} + F_{rr} + F_D(x) \quad (10)$$

$$F_D(x) = (A(x) + B(x)\ S + C(x)\ S^2)\ f_i\ W(x)\ 100\ D_T(x) + F_{MR} \quad (11)$$

$$F_{MR} = F_N \frac{\left(\frac{1}{B_n} + 0.04 + \frac{0.05\ s}{\sqrt{B_n}}\right)}{1000} \quad (12)$$

where $F_D(x)$ is draft force requirement for field work task x, $P_{Field}(x)$ is total power requirement for task x, f_i is a dimensionless soil texture adjustment parameter, A, B and C are machine parameters, v is the vehicle's speed in m s^{-1}, S is field speed in km h^{-1}, W is implement width for task x in m (or in no. of tools), D_T is tillage depth in m, F_{MR} is motion resistance in kN, s is decimal slippage and B_n is a dimensionless ratio depending on wheel parameters and soil type.

Five of the seven field operations were calculated using this method. The other two, fertiliser spreading and pesticide spraying, were calculated using empirical data taken from Lindgren, Pettersson, Hansson, and Norén (2002), who measured the power requirements for different operations by multiple tractors in the field during a growing season. Spraying was not measured in that study, so measured values for spraying recycled urine under good conditions were used in the model instead. Empirical values for ploughing, cultivation, sowing, roller packing and harrowing taken from Lindgren et al. (2002) were also used to validate the model (Fig. 4). It was assumed that the battery would always need recharging before any spraying tank or fertiliser bin was empty and that tank/bins were refilled on the farm while the battery was recharging or being replaced, and therefore no separate modelling was needed.

The rate at which the tractor could perform each operation was calculated according to Witney (1988):

$$C_o(x) = \frac{W(x) S \eta_{Field}}{10} \quad (13)$$

where C_o is the overall rate of work for task x in ha h^{-1}, η_{Field} is a decimal field efficiency factor due to sub-optimal field geometry and implement width, and 1/10 is a conversion unit for km m h^{-1} to ha h^{-1}. All calculated C_o values are shown in Table A.2.

The tractor remained in the field until the current task was completed or the battery energy reached a pre-set threshold of the sum of θ_{min} and the additional energy needed for transport back to the farm. When one of these was triggered, the vehicle returned to the farm for recharging and to prepare for the next field or operation. If the tractor left the field with more battery energy than the threshold, this resulted in a correspondingly shorter charging time, as described in section 2.7.1. The behaviour of the battery during work in field n and the thresholds for exiting can be described as follows:

$$\theta(t) = \theta(t_0) - \frac{P_{Field}}{E_B} t;\ \ \theta_{min} + \frac{E_{Road}(n)}{E_B} \leq \theta(t) \leq \theta_{max} \quad (14)$$

where t_0 denotes the simulation time (h) when field work started.

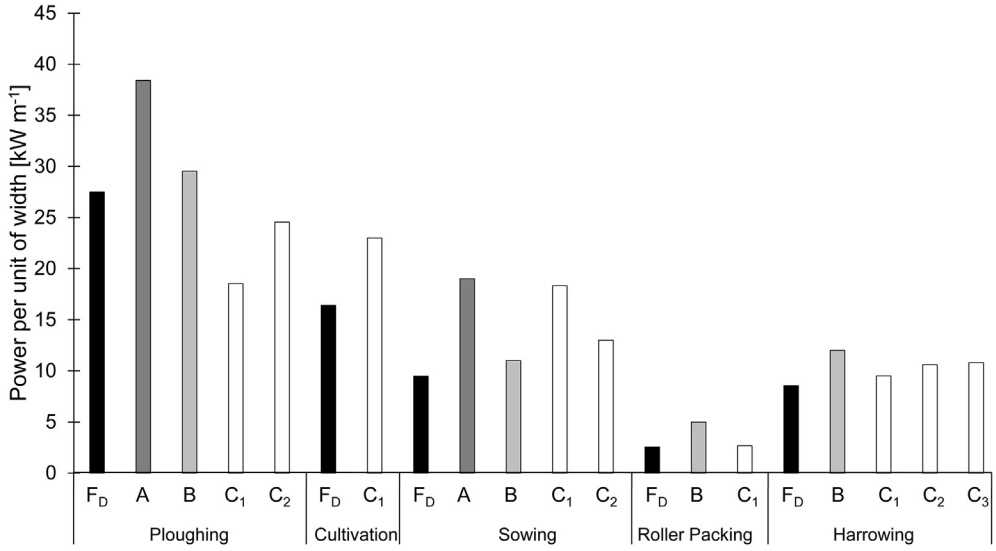

Fig. 4 – Comparison of calculated draft power requirement based on ASAE (2000) and measured values (Lindgren et al., 2002). Draught force (F_D) is the calculated value used in the model, other bars represent measured values for different tractor models: Case 240 IH Max (A), Valtra 6650 (B) and Valtra 6600 (C_i).

2.7. *Charging system and battery*

2.7.1. *Charging system modelling*

The BEV was assumed to use one of two charging methods; conductive charging (CC) as described in Yilmaz and Krein (2013), or a battery exchange system (BES) where the entire battery pack is replaced, as described in Cheng, Chang, Lin, and Singh (2013) and Kim, Song, and Choi (2015). When the battery was replaced in the BES, the empty battery was assumed to be recharged with CC while the tractor returned to work with a fully charged battery pack, meaning that the BES still needed a CC system. The time required for replacement of a battery pack was set to a constant 10 min. Shorter changing times have been reported for cars by Tesla and Better Place (Adegbohun, von Jouanne, & Lee, 2019; Afonseca, 2018) and times down to 60 s for large battery packs in buses (Kim et al., 2015). Here, a higher changing time was set to give a margin of error.

For the CC system, the vehicle acquired a resource labelled *charger* (of the N_C available) in the model and then proceeded to charge up to the threshold shown in Equation (15). If no charger was available, the vehicle was placed in a queue until a charger was available. When a battery was fully charged, it released its charger for further use. The BES was modelled in a similar way to the mixed queue network used by Tan, Sun, Wu, and Tsang (2018), also using multiple coupled queues for different resources (vehicles, batteries etc.). In the present model, the vehicle first acquired a fully charged battery in the form of a resource labelled *battery* (of the N_B available) and waited the fixed battery replacement time before exiting fully charged. The empty battery acquired a *charger* resource and charged via CC, and when this was done the battery resource was made available for the next vehicle as a fully charged battery.

The process of CC battery recharging can be approximated by a linear increase in SoC over time. This linear method can be an adequate fit for some methods of charging at certain intervals of SoC, in this study for the CC/CV method (constant current/constant voltage (CC/CV), as described by Shen, Tu Vo, and Kapoor (2012)), for SoC between 0.2 and 1. This has been used in calculations and modelling in several studies (Hamidi, Ionel, & Nasiri, 2015; Harighi, Bayindir, & Hossain, 2018; Klein et al., 2011).

The simulated behaviour of $\theta(t)$ during charging via CC can be described as follows:

$$\theta(t) = \theta(t_0) + \frac{P_c\ \eta_{charger}}{E_B} t;\ \theta_{min} \leq \theta(t) \leq \theta_{max} \quad (15)$$

The tractor remained at the charger until $\theta(t)$ was equal to θ_{max}. The tractor was then released. Both of the recharging methods, CC and BES, in the BED system were simulated to take place on the main farm.

2.7.2. *Battery modelling*

As the focus of the simulation was to identify general relationships and patterns, the battery was modelled as an internal system with the function of an energy reservoir. The dynamic SoC-level, $\theta(t)$, was the only internal battery variable that varied dynamically during the simulation, even though energy use was also measured. Use of $\theta(t)$ as the only state-variable in simplified battery models has been described previously, by e.g. Tremblay, Dessaint, and Dekkiche (2007) and Grunditz and Thiringer (2016). The battery had a set restriction where the SoC-level could not go below θ_{min}, to avoid deep discharge damage and ensure adequate operational life time. To achieve this, how much energy would need to be reserved for transportation to and from the field (E_{Road}) was predicted. The remaining part of the battery energy was used for field work (Fig. 5).

For CC, the battery was modelled as using a simplified method for discharging where $\theta(t)$ decreases linearly with time. It was assumed that the battery was able to receive charging power and power the motor without constraints, regardless of size. It was also assumed that the battery was

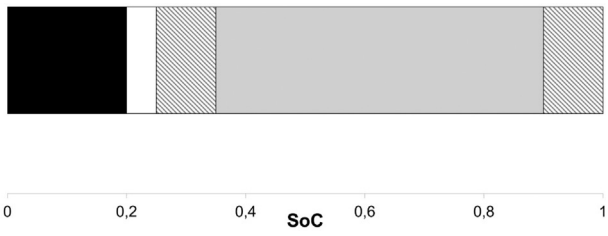

Fig. 5 – Example of state of charge (θ) distribution of the modelled battery in: field work (grey), road transport (diagonal), θ_{min} (black) and losses due to non-perfect efficiency (white).

new and unused at the start of the simulation. Battery deterioration and resulting loss of capacity was omitted from the model, even though it is of great interest and it should be included in future studies.

2.8. Diesel system

To make comparisons against conventional agricultural vehicle systems, the model was modified to simulate diesel tractors with the same vehicle power (P_V) and number of vehicles (N_V) as the simulated BEVs. Two cases were simulated; an autonomous diesel tractor operating 24 h d^{-1} and a diesel tractor operating for 10 h d^{-1}, the latter simulating a conventional manned vehicle. The 10-h version was constrained to never work more than 10 h d^{-1}, but could start at different times of the day, depending on the weather.

The main differences were replacing the battery with a diesel tank and the charger with a diesel pump, and changing the engine efficiency to match ICE levels. Data on diesel tank volume were for the CLAAS ATOS (55–79 kW) series of tractors (CLAAS, 2018). The diesel tank was assumed to carry 130 l of diesel, corresponding to a battery of 1315 kWh, which was used as E_R for the diesel systems as it was assumed that no losses occurred in the tank and that all diesel was used. The electric charging was replaced with a diesel pump with a flow rate of 50 l [diesel] min^{-1}. This corresponds to the energy flow in an electric charger of 30.3 MW, which was used as P_C for the diesel systems. It would give a refuelling time of <3 min, which made having more than one fuel pump redundant, so N_C was set to 1. The engine efficiency of combustion engines is non-constant in real use, but in this simulation it was set to a constant 30%, which corresponds to an average to high value for smaller agricultural tractors (Wasilewski et al., 2017).

2.9. Simulation inputs and base case configuration

A base case configuration was chosen as a basis for comparison, with the criterion that the resulting mean time needed for field work in the spring period (T_{Spring}) should be roughly 30 days or less for the 30-year period 1989–2018. In the model, the spring period is the most time-consuming and time-sensitive period. It is also of high importance for the remaining cropping period. Multiple configurations could

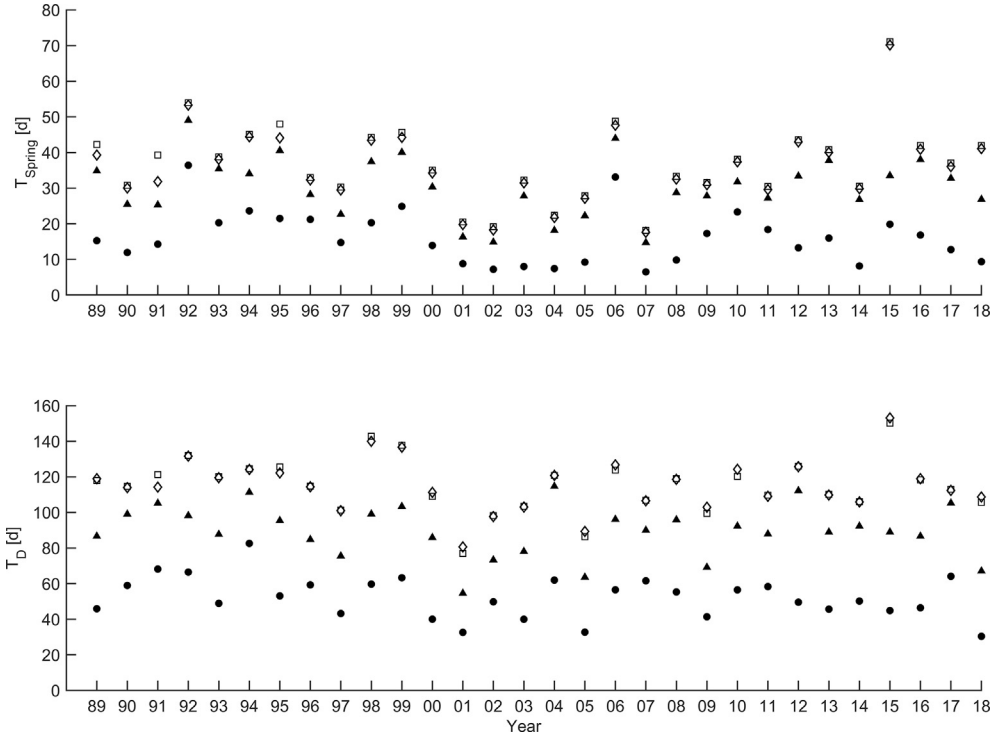

Fig. 6 – Distribution of total active time (T_D) and total active time during spring (T_{Spring}) for the base case configuration over 30 individual years, compared with the corresponding configuration for a battery exchange system (BES). T_{Spring} is calculated from the first workable hour of the spring period, not from the simulation start. Conductive charging (CC) (□), BES (◊) and diesel systems with 24-h (•) and 10-h (▲) working periods are shown.

Table 4 – Average value, median and standard deviation for total active time (T_D) and total active time during spring (T_{Spring}) for the base case configurations (see Table 3) in two battery electric drive (BED) systems (conductive charging (CC), battery exchange system (BES)) and two diesel tractor systems with different work periods (10 or 24 h d^{-1}), 30-year sample size.

	T_D				T_{Spring}			
	CC	BES	Diesel (10)	Diesel (24)	CC	BES	Diesel (10)	Diesel (24)
Average	115.2	115.4	89.7	52.3	37.2	35.0	30.2	16.1
Median	116.4	114.3	89.5	51.7	37.6	35.1	29.5	15.0
Std. Dev.	15.1	14.9	14.3	11.5	10.9	10.7	8.3	7.3

meet this criterion, but the base configurations shown in Table 3 were chosen as they were compatible with the aim of the study by allowing multi-vehicle system dynamics to be considered. Both modes of recharging in the BED systems were simulated using the base case configuration. In addition, the diesel systems were simulated for comparison with the same inputs; apart from P_C and E_R as described in section 2.8. The different inputs were chosen as they all represented different solutions that exists on the market today or have been studied previously. Furthermore, they were chosen to be reasonable for the economy and fuse size of a farm of the given size.

3. Results

3.1. *Base case configuration results*

Simulating the base case scenario for 30 different years (1989–2018) gave the T_{Spring} and T_D values shown in Fig. 6 for CC, BES, diesel with a 10-h working day and diesel with a 24-h working day.

The difference between years was significant and reflects weather dependency, as only the weather data varied between the years. Using BES always resulted in lower T_D and T_{Spring} than using CC for this configuration (Fig. 6), although the difference was small. For the spring period, the 10-h diesel system had shorter T_{Spring} than both the BES and CC systems, with a median value of 3.8 d. When considering the entire year, the 10-h diesel system had consistently shorter T_D than the BED systems, because of the more demanding field work done in autumn (ploughing and power cultivation). The average and median values for the entire 30-year period are shown in Table 4.

Compared with CC, the average T_D with BES was 0.2 d longer, while T_{Spring} was 2.2 d shorter. However, the median values showed that BES was 2.5 and 2.1 days shorter for T_{Spring} and T_D, respectively. The 24-h diesel system resulted in the shortest average T_D, 52.3 d. With the 10-h diesel system, T_D increased to 89.7d. The average time distribution for the different base cases is shown in Fig. 7. Apart from different T_D, a shift in the distribution was also noted between the cases.

The average time spent on road transport per vehicle was similar between the two modes of recharging in BED systems (11.6 d for BES and 12.1 d for CC). This was unsurprising, as the

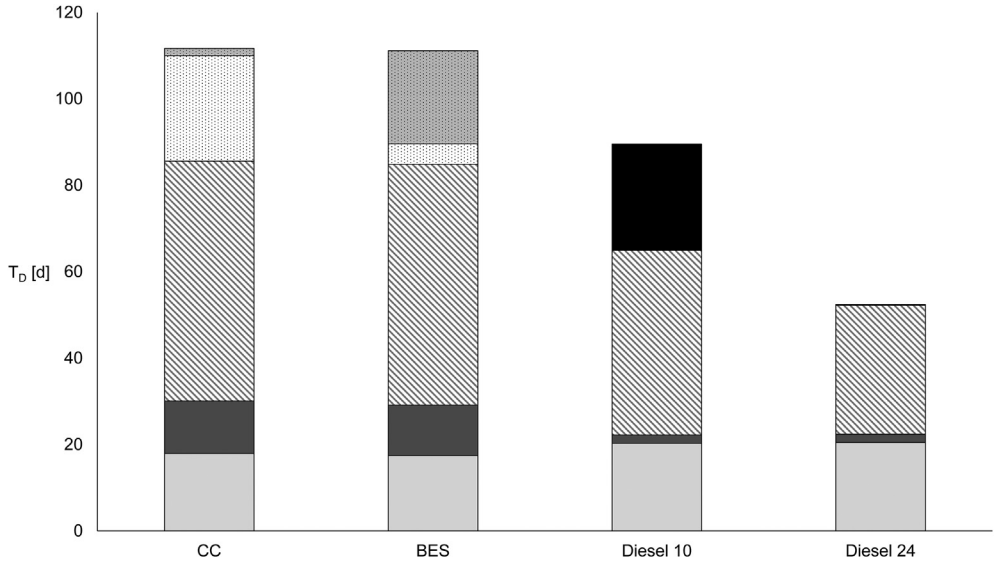

Fig. 7 – Average time distribution per vehicle for the base case for different charging methods (battery exchange system (BES), conductive charging (CC)) and for two diesel systems with different work periods (10 and 24 h). Charge (white dotted) denotes all types of refuelling, charge queue (grey dotted) is the time spent queuing for refuelling, weather (white diagonal) is the time spent waiting for improved soil workability, transport (dark grey) is the time spent in transit between farm and field, and field work (light grey) is the time spent doing field work. For the 10-h diesel system, rest (black) denotes the time outside the working schedule of a driver.

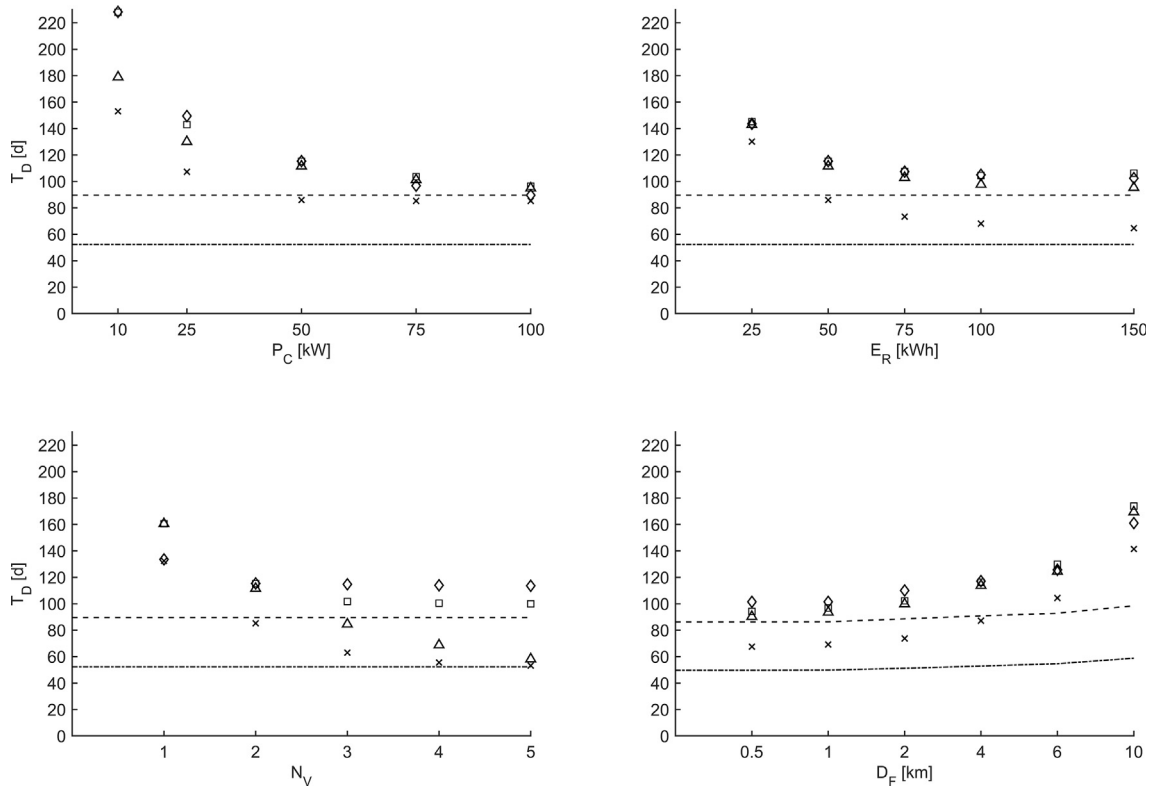

Fig. 8 – Change in total active time (T_D) in response to changes in: charger power (P_C, top left), battery energy content (E_R, top right) and number of vehicles (N_V, bottom left), with all other parameters set to the base case configuration ($N_V = 2$, $N_C = 1$, $N_B = 1$, $E_B = 50$ kW h, $P_C = 50$ kW). Variable distance from field to farm (D_F, bottom right) is also shown for all cases. CC (□) = conductive charging, BES (◊) = battery exchange system. CC*(Δ) and BES* (X) are configurations with no or minimal charging queues, for comparison with a better optimised system. The two diesel systems, 10-h (dash-dotted line) and 24-h (dashed line), with $N_V = 2$, are also displayed for comparison.

time in transit depended on the number of times recharging was required. This in turn depended on the battery capacity, which was equal between the modes. Since the time spent refuelling and in transit was dependent on the energy carried by the vehicle, the two diesel systems spent a low fraction of their time on both, 1.95–1.96 d vehicle^{-1}. The amount of time spent working was roughly equal between the cases (17.5–20.5 d vehicle^{-1}, 35.0–40.9 d total), as a certain amount of fixed work was needed to complete all tasks, but the fraction of total time spent on field work varied greatly, from 16% for BES to 39% for the 24-h diesel system. The BED systems spent slightly less time working in the field due to their higher driveline efficiency compared with the diesel systems. The time spent waiting for acceptable weather, and by extension field workability, was a large fraction (48–57%) of the total time for all systems. The time spent waiting for acceptable weather varied between the systems, from 29.8 to 55.7 d, but the fraction was similar in all cases.

Comparing CC and BES, the main difference was in the time spent charging. The time saved on charging for BES constituted the difference in T_D between the systems. Optimising the BES configuration to avoid charging queues could give a further 19.9 d reduction compared with CC, as queueing took up 82% of the total time spent recharging for the BES. Although N_C and P_C were equal between the modes, BES had a larger queue time fraction than CC, implying a scheduling problem with charging, i.e. greater risk of multiple vehicles returning for recharging at the same time, creating queues.

It is important to note that, even though the states are mutually exclusive, time spent in one can reduce the time spent in another, see Fig. 7. For example, time spent charging in the CC system could be time that would otherwise be spent waiting for better weather, or in the 10-h diesel system the workability control comes before the daily working time control, meaning that time spent waiting for better workability would otherwise have been spent waiting for the working day to begin.

3.2. *Variable input influence*

In addition to the base case, simulations were run with the inputs shown in Table 3 and where P_C, E_R and N_V were all varied from the base case separately, for both recharging systems and both diesel systems (Fig. 8). For the BED systems, both the series with the base case configurations and more optimal systems in terms of N_B and N_C were included.

Charger power (P_C) was influential for both CC and BES, decreasing T_D when increased to 75 kW where the number of chargers could successfully service all vehicles. Further increases gave only a limited effect. For the optimised BES, a maximum P_C of 50 kW sufficed, provided enough chargers and batteries were available. For $P_C < 50$ kW, CC had a lower T_D compared with BES, while BES had lower T_D in every other case.

Rated battery energy content (E_R) had a similar effect on both systems, with a decrease in T_D with increased E_R, and subsequently E_B. For CC, this was characterised as a diminishing return, since a larger E_R meant more fieldwork before recharging, but also longer charging times that counteracted the gains. This is evident in Fig. 8, where the optimised CC system was only slightly better than the base case for all battery sizes. Further gains required an increase in P_C in addition to increases in E_R to keep the charging time low. For BES the benefits were more direct, as a large E_R did not necessarily correlate with a longer charging time. As long as a fully charged battery was available when the tractor returned for recharging, a larger E_R simply meant more time for field work. This is seen in the large difference between the base case configuration and the optimised system for BES in Fig. 8.

Increasing N_V led to lower T_D, especially for the optimised systems. $N_V > 2$ led to T_D that was lower than for the manned diesel system, and a higher number of vehicles could compete with the unmanned diesel system. The distance between farm and field (D_F) was also varied, as can be seen in Fig. 8. For the diesel systems this parameter had a low impact on T_D, with a difference of 9.2–12.2 d between $D_F = 0.5$ and $D_F = 10$ km. In comparison the T_D of both CC systems and the non-optimised BES was highly impacted by an increase in D_F, with an increase of 73.8–79.6 d when D_F increased from 0.5 to 10 km. An optimised BES was less affected and showed an increase of 59.6 d under the same inputs. For $D_F > 4$ km, both BES performed better than their CC counterparts.

The results of varying number of chargers (N_C) for different P_C and E_R of the CC system are shown in Fig. 9. An increase in N_C gave a benefit in terms of lowered T_D until elimination of queues, after which a further increase gave minimal benefit. As can be seen in Fig. 9, an increase in N_C was most effective with lower charger capacities, while at higher P_C an increase yielded no improvement, as the charger need was already met by faster chargers. While N_C affected T_D for different battery sizes, the effect was less pronounced than that of charger power.

For the BES, some notable patterns emerged, as shown in Fig. 10. Increasing P_C, N_B or N_C was only beneficial up to the point where queues and general waiting time could be avoided. Increases beyond that point had no or minimal benefit on T_D, most notably seen at $N_B \geq 2$ (Fig. 10). Similar findings were obtained for other configurations of the BES.

3.3. *Energy and time consumption*

Energy consumption for the different base cases was measured and compared with that in other studies on similar crops and environments (Daalgard, Halberg, & Porter, 2001; Kitani et al., 1999; Chaston, 2008; Lindgren et al., 2002; Safa, Samarasinghe, & Mohssen, 2010; Wells, 2001; Witney, 1988). Fuel consumption data for field operations from these sources were used in calculations for the spring wheat rotation shown in Fig. 11, where simulated energy use is converted to equivalent litres of diesel. This was done using a density of 845 kg m^{-3} and a net calorific value of 43.1 MJ kg^{-1} was taken from Reif and Dietsche (2014) which is in accordance with the European Union standard for diesel fuels, EN 590. The simulated energy use was obtained through the following equation of energy as a function of the integrated sum of powers for each vehicle N_i and task x:

$$E = \int_0^t \frac{\sum P(N_i, x)}{\eta_{Motor}\ \eta_{Transmission}} dt \quad (16)$$

where η_{Motor} is the decimal average motor efficiency.

The results showed that the energy consumption for the BED systems was 58.0% lower than for the corresponding

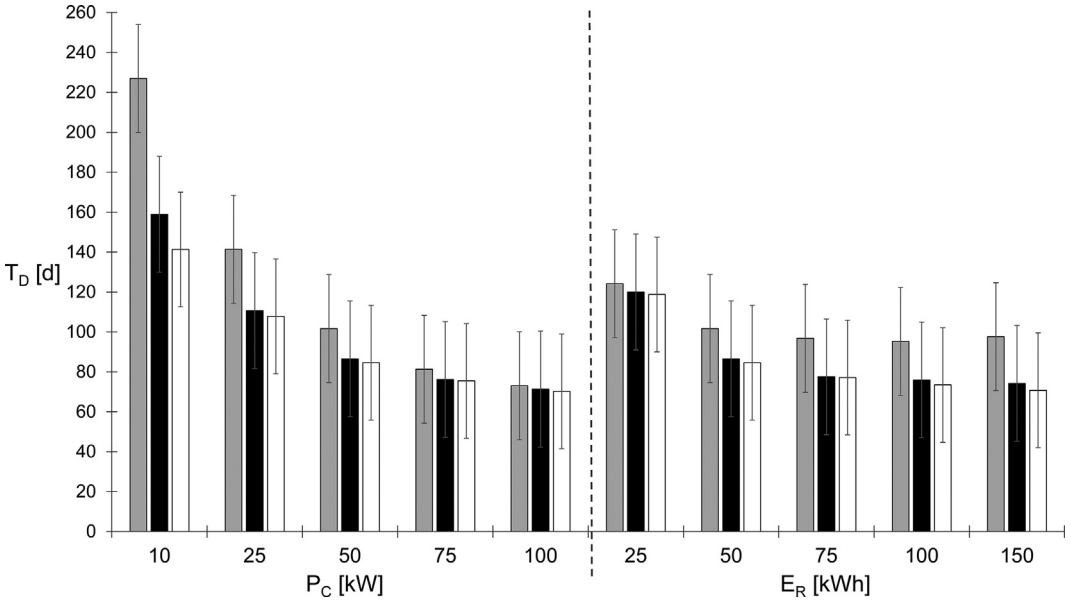

Fig. 9 – Total active time (T_D) for different configurations where number of vehicles, $N_V = 3$ for conductive charging (CC) and charger power (P_C, left) and battery energy content (E_R, right) are varied. All values are 30-year averages, error bars show 2 SDs. On the left $E_R = 50$ kW h and on the right $P_C = 50$ kW. Number of chargers (N_C) 1 (grey), 2 (black) and 3 (white).

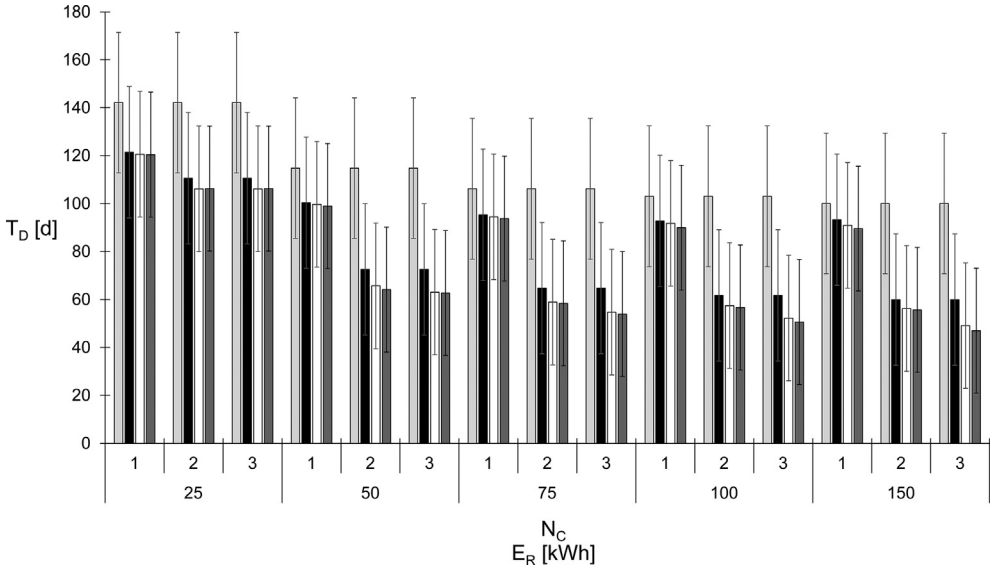

Fig. 10 – Total active time (T_D) for different configurations of number of additional batteries (N_B, columns), number of chargers (N_C, top x-axis) and battery energy content (E_R, bottom x-axis) in the sub-set for the battery exchange system (BES) where number of vehicles $N_V = 3$ and charger power $P_C = 50$ kW. All values are 30-year averages, error bars show 2 SDs. The columns show number of batteries $N_B = 1$ (light grey), 2 (black), 3 (white) and 4 (dark grey).

simulated diesel systems' and 45.8% lower than average empirical values presented previously for similar soil type and weather conditions (Lindgren et al., 2002).

The total time required for each hectare was measured for all cases by normalising the time spent doing fieldwork and transport, in hours, over the total area. For the base case, CC had an average time requirement of 7.8 h ha^{-1} and BES a requirement of 7.7 h ha^{-1}. The time requirement for the diesel systems with 10 and 24 h working time was 5.3 ha^{-1} in both cases.

4. Discussion

4.1. General results

There was a non-negligible difference between BES and CC in terms of active time, with BES resulting in lower T_{Spring} and T_D in the majority of years for the base case configurations. In addition, a well-optimised BES was consistently as good as, or

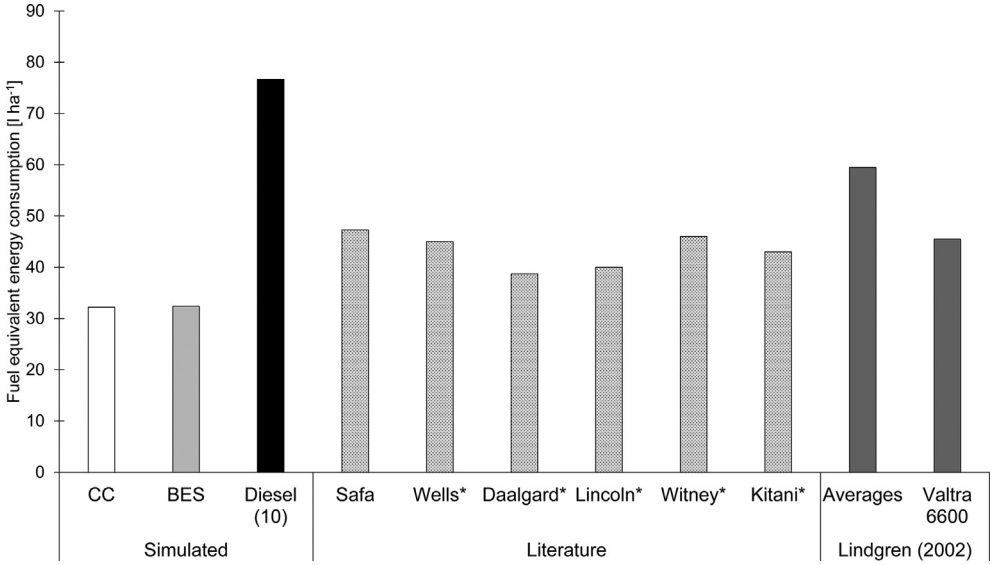

Fig. 11 – Fuel consumption per hectare for a spring wheat cropping system. Comparative values from literature sources on consumption for specific operations and the 30-year average simulated base cases for battery exchange system (BES), conductive charging (CC) and diesel (10-h day). Road transport was not included in the literature sources and data on roller packing were missing from the marked sources (*), so these were omitted from the calculations. Fuel consumption during harvesting was omitted in all cases.

better than, a corresponding CC-system for all configurations. Since the aim of the study was to compare the different charging methods with each other and equivalent diesel systems, the choice of T_D and T_{Spring} were deemed adequate as an indication of which system performed better. In further studies, more in-depth comparisons featuring scheduling, timeliness and time management optimisation are encouraged as they fell outside the scope of this study.

For CC systems, increasing N_C was only relevant when there was a queue to the chargers, which only occurred when low P_C was paired with high E_B. Increasing P_C had less of a diminishing return than increasing E_B, since larger battery capacity meant longer field work runs, but also longer charging times, while increased P_C only yielded shorter charging times. An increase in P_C always yielded a greater improvement in T_D than adding more chargers (i.e. one 50 kW charger resulted in lower T_D than two 25 kW chargers, even though the total charging capacity was the same). This indicates that for CC, few large chargers were better than multiple less powerful chargers. The BES was more flexible and there was no definitive better option. This is best shown in Fig. 8, where a well optimised BES with $P_C = 50$ kW had a lower T_D than the corresponding CC system with $P_C = 100$ kW. For CC, periods of time spent charging coincided with bad weather where the tractor would be unable to work regardless, thereby mitigating the disadvantage of longer charging time compared with BES.

For BES, increasing P_C was only efficient up to the point where queues to a fully charged battery were eliminated, after which no further advantage was gained from increasing the available power. This is similar to the dynamics found by Tan et al. (2018) in their simulation of a BES, particularly for variables N_B and N_C. In contrast, for the CC system larger P_C always proved beneficial, albeit with diminishing returns. For BES, larger batteries proved increasingly beneficial up to the point where the chargers could not provide fast enough charging to avoid queues. Furthermore, after increasing the battery capacity to a high enough level to complete any task in any field, any further benefit was lost as the vehicle was assumed to return to the farm after each field. However, this is a constraint of the simulation and real-world use would derive greater utility from such a battery. The BES also had a flat battery changing time of 10 min on top of the time it took to charge the batteries, which can explain why, for lower D_F, BES had a higher T_D than CC. In most other scenarios this time was small compared with the charging time of the CC system, which resulted in BES being the faster system in those cases.

Increasing the number of vehicles correlated directly with an increase in rate of work (C_o) and was an efficient way of reducing T_D, although again with diminishing returns. For both CC and BES, it was important to increase other variables along with the number of vehicles, as charger capacity and battery availability quickly became bottlenecks and further increases in vehicle numbers yielded no benefits (see Fig. 8). The behaviour of the BED systems with increasing D_F indicates that, due to the frequent recharging of battery systems, they are better suited to an environment where recharging infrastructure is as close as possible, to minimise transport time. For $D_F > 4$ km, both non-optimised BED systems had difficulties completing all operations, especially as heavy tillage required frequent recharging due to the heavy nature of the work. For BES the possibility of bringing multiple batteries to the field exists, and $D_F = 0.5$ km gives a good indication of the optimal benefits of this solution, even though this option was not explored in the present study. The results indicate that it could be a feasible option for fields far away from recharging infrastructure, provided that battery exchange can be facilitated on-site.

The modelled system assumed a heavy tillage cropping system on clay-rich soil in a wet temperate climate, which is energy-intensive and demanding on BED vehicles. This study modelled and simulated a conventional cereal system, with the assumption that BEDs would replace ICE tractors for every activity, without altering the tasks or crops. A simplified and static vehicle model was also assumed. The values obtained for fuel consumption and work rate were similar to those found in other sources, but further research and simulations of vehicles, other environments, soils and cropping systems, and more detailed simulations of vehicles could improve understanding of the benefits and restrictions of these kinds of systems. Ideally, field tests would be a good complement.

4.2. *Workability and weather*

Weather was highly influential, with on average 50.7% of the active time of the year spent waiting for better workability in fields. In this study, no account was taken of the relationship between vehicle weight and workability. Smaller, often lighter, machines were considered and they would probably have a larger window of workability than larger machines. The limit for trafficability (defined as the capability to support agricultural traffic and not harm the soil or ecosystem), and the potential gains from reduced soil compaction were also omitted from the analysis, even though these are arguably among the greatest advantages of smaller vehicles. Further research is required in this area.

In the model, it was assumed that all fields were uniform and identical as regards soil parameters and soil type. This is a simplification, as these parameters can vary between neighbouring fields and even within fields. Hydraulic conductivity in particular is known to vary in-field (Nilsson, Larsolle, Nordh, & Hansson, 2017), but was assumed here to be constant and uniform, following Witney (1988). As weather and soil workability was not the main focus of the study, this simplification could be acceptable. Another assumption was that the control for the workability criterion was made on the farm and, if met, the vehicle completed a run before returning. However, the difference between the simulated fraction of time spent queueing for better workability and the calculated fraction of time when the soil was too moist to be workable was generally small (+/−5% of the time spent waiting in an average year), which indicates that this assumption had a limited impact on the results.

The predicted workability for a certain period was estimated for time steps greater than 1 h. Both de Toro and Hansson (2004) and Nilsson and Bernesson, (2009) predicted workability for a certain day and Witney (1988) suggested predicting the number of working days per month or quarter. Increasing the resolution to hours might lead to a harsher assessment of workability. Daily variations in temperature or

moisture (night–day cycle and dew accumulation) were not implicitly included in the model, which for a resolution of days might be accurate but for a resolution of hours might be a simplification. The proportion of time appropriate for field work reported in different studies varies, with most citing 55–70% (de Toro & Hansson, 2004; Nilsson, 1976; Witney, 1988). In this study, the value was on average 48%. A value more consistent with the literature might have been more lenient towards BED systems, as weather was the greatest cause of non-productive time. Apart from the weather in the different years, changing the workability criterion would have had a noticeable impact on the amount of time spent waiting for better workability status. A more lenient criterion would have permitted a larger number of feasible configurations.

4.3. *Fixed power and scalability*

The power of the vehicle was kept fixed in simulations, as the focus was the charging systems and the general dynamic relationship between BEV and autonomous vehicles. Larger, or smaller, vehicle power would have a noticeable effect that would vary with different mode of use and for different farms, but was not simulated here. The complexity of encompassing all field work operations leads to a problem of optimisation and this article chose to focus on smaller vehicles than the current diesel tractors. Other vehicle concepts such as Thorvald II (Grimstad & From, 2017) solve this by being modular, while the Fendt Xaver (Fendt, 2017) and the TERRA-MEPP (Young et al., 2018) are small, specialist vehicles of lower complexity than an all-operation vehicle and they avoid heavy tilling operations altogether. In future studies, a "ploughing-free" or "no-till" work cycle would be interesting to investigate, as BED systems could be assumed to fit better there than in a conventional work cycle including heavy tillage.

Scalability of the systems is an area of interest for future studies. Systems of the kind studied here might not be used primarily on farms of moderate size, but on larger farms with greater ability to invest in new technology and a greater need for hired manpower. Logistics is a greater bottleneck for farms with large field area and long transport distances than for farms with smaller field area (Engström et al., 2015). In previous studies, field size and shape (Nilsson, Rosenqvist, & Bernesson, 2014), road transport distances (Engström et al., 2015) and total field area have been described as important parameters. Thus analysis of other total field sizes, layout, motive powers and total farm area would be interesting in future research.

5. Conclusions

Dynamic simulation results indicated that autonomous BEV in both BES and CC systems could be similar to conventional manned diesel tractors of corresponding sizes in terms of yearly active days required. This was shown for battery energies significantly smaller than the contents of a diesel tank and at charger powers that are feasible for the fuse size of small-medium Swedish farms, with the lower work rate and less on-board energy of BEDs being offset by autonomous operation. It was also shown that the simulated BED systems had lower energy consumption per hectare than the simulated diesel systems (58% lower) and literature values for diesel systems (17–46% lower).

In base configuration simulations, spring operations were completed in 37.2 d on average for CC and 35.0 d for BES; an improvement of 2.2 d. The average total active yearly time required was 115.2 d for CC and 115.4 d for BES in the base case, while the average values for well-optimised systems showed that BES was 25.7 d faster than CC ($T_{D(CC^*)} = 111.6$ d, $T_{D(BES^*)} = 85.9$ days) and the manned diesel system ($T_{D(Diesel10)} = 89.7$ d). Choosing BES over CC for similar configurations lowered the required time in all cases except for $P_C < 50$ kW. When multiple chargers or batteries were available, BES consistently performed better than CC. These results indicate that the BES simulated performed better than the CC system on average and as an optimised system. The number of calendar days needed to conduct the necessary work varied asymptotically with component size (i.e. charger power, battery capacity; see Fig. 8). As long as the capacity was enough to avoid bottlenecks, adding extra capacity provided limited improvement. However, when the component sizes were too low, the number of calendar days increased rapidly.

The difference in total active time between the BES and CC systems was small for most of the configurations compared, but BES consistently needed the same or less time to complete all operations than similar CC systems. For both systems, charging queues proved detrimental. As both BED systems generally had a lower rate of work due to frequent recharging than conventional diesel systems, it was important to maximise the time available for field work. Due to the frequent recharging and lower recharging speed, the BED systems spent more time in transit and recharging than the diesel systems, meaning the BED tractors are better suited for farms with their fields nearby. It proved important with a good understanding of the sources of non-productive time. The non-productive time could be reduced by reducing queueing through increasing the battery capacity (providing a longer time between recharges), increasing the charger capacity (decreasing the charging time), scheduling the vehicles to avoid queues, or using non-productive time (mainly waiting for better workability) to charge the vehicle batteries.

Declaration of Competing Interest

The authors declare that they have no known competing financial interests or personal relationships that could have appeared to influence the work reported in this paper.

Acknowledgements

This work was funded by the Swedish Government research programme "STandUP for Energy" and the Swedish Energy Agency under grant number P44831-1.

Appendix A. Parameter Values and Constants

Table A.1 – Model constants and values used in simulations

Parameter	Description	Value	Source
A	Vehicle front area (m^2)	2	
a	Acceleration ($m\ s^{-2}$)	2	
B_n	Machine/soil ratio parameter	55	ASAE (2000)
C_D	Drag coefficient (decimal)	0.9	Reif and Dietsche (2014)
C_{rr}	Rolling resistance coefficients (decimal)	0.1 (field) 0.1 (road)	(Witney, 1988) Reif and Dietsche (2014)
FC	Field capacity of soil ($mm\ m^{-1}$)	89.8	Witney (1988)
F_N	Normal force (N)	31,392	$g = 9.81\ m\ s^{-2}$
m	Mass (kg)	3200	
S	Field speed, mean ($km\ h^{-1}$)	5	Witney (1988)
S_{Road}	Road speed, mean ($km\ h^{-1}$)	22.1–33.1	Varies with D_F (n)
s	Slippage (decimal)	0.2	ASAE (2000)
θ_{min}	Minimum allowed state of charge (decimal)	0.2	
θ_{max}	Maximum allowed state of charge (decimal)	1.0	
α	Gradient (%)	10	
η_{Field}	Field efficiency (decimal)	0.8	Witney (1988)
η_{Motor}	Motor efficiency (decimal)	0.95 (BED) 0.3 (ICE)	(Andersson, 2019) (Wasilewski et al., 2017)
$\eta_{Transmission}$	Transmission efficiency (decimal)	0.85	(Ryu, Kim, & Kim, 2003; Serrano, José, da Silva, Pinheiro, & Carvalho, 2007)
$\eta_{Battery}$	Battery efficiency (decimal)	0.97	
$\eta_{Charger}$	Charger efficiency (decimal)	0.95	Lucas, Trentadue, Scholz, and Otura (2018)
ρ_{air}	Density of air ($kg\ m^{-3}$)	1.225	Reif and Dietsche (2014)

Table A.2 – Constants and implement parameters used for calculating draft implement force (F_D) and power (P_D), ordered by task (ASAE, 2000)

Task (x)	f_i	A	B	C	D_T [m]	W[a] [m]	F_D [kN]	P_D	C_0 [ha h^{-1}]	Range +/− %
Cultivation (Field cultivator)	1	46	2.8	0	0.10	2.6	9.98	33.6	1.0	30
Harrow (Spring-tine harrow)	1	2000	0	0	0.01	5	9.18	13.9	2.0	30
Roller packer	1	600	0	0	0.01	12.3	14.58	10.3	4.9	50
Sowing (Grain drill)	1	300	0	0	0.01	3.0	19.50	6.3	1.2	25
Ploughing (Mouldboard plough)	1	652	0	5.1	0.20	1.55	17.60	33.6	0.6	40
	P/W [kW m^{-1}]	P_D	W [m]	C_0 [ha h^{-1}]						
Fertiliser spreading	3.12	17.2	24	9.6						
Pesticide spraying	2.29	17.2	24	9.6						

[a]Maximum implement width based on the largest available implements for the chosen vehicle power, from the manufacturer Kvarneland and retailer Lantmännen Maskin at time of publication.

REFERENCES

Adegbohun, F., von Jouanne, A., & Lee, K. (2019). Autonomous battery swapping system and methodologies of electric vehicles. *Energies, 12*(4). https://doi.org/10.3390/en12040667.

Afonseca, A.d. (2018). *Simulation of charging systems for electric autonomous agricultural vehicles*. M.Sc Master Thesis. Swedish University of Agricultural Science. Retrieved from urn:nbn:se:uu:diva-354885 (ISSN 1401-5765).

AgroIntelli. (2019 March 2019). Robotti - a powerful tool to increase agricultural productivity. Retrieved from http://www.agrointelli.com/robotti-diesel.html.

Alcock, R. (1983). Battery powered vehicles for field work. *Transactions of the Asae, 26*(1), 10–13. Retrieved from <Go to ISI>://WOS:A1983QC76300003.

Andersson, R. (2019). *On the design of electric traction machines - design and analysis of an interior permanent magnet synchronous machine for heavy commercial vehicles*. PhD Doctoral Thesis. Lund, Sweden: Lund University. Retrieved from http://portal.research.lu.se/portal/files/55630852/On_the_Design_of_Electric_Traction_Machines.pdf.

ASAE. (2000). *Agricultural machinery management data (ASAE D497.4)*. 2950 Niles rd., St. Joseph, MI 49085-9659, USA: American Soceity of Agricultural Engineers.

Bawden, O., Ball, D., Kulk, J., Perez, T., & Russell, R. (2014). *A lightweight, modular robotic vehicle for the sustainable intensification of agriculture. Paper presented at the Australian conference on robotics and automation (ACRA 2014)*. Melbourne, VIC: University of Melbourne. http://www.araa.asn.au/acra/acra2014/papers/pap147.pdf.

Case IH Agriculture. (2019). *Autonomous concept vehicle*. Retrieved from https://www.caseih.com/northamerica/en-us/Pages/campaigns/autonomous-concept-vehicle.aspx.

Cheng, L., Chang, Y., Lin, J., & Singh, C. (2013). Power system reliability assessment with electric vehicle integration using battery exchange mode. *IEEE Transactions on Sustainable Energy*, 4(4), 1034–1042. https://doi.org/10.1109/tste.2013.2265703.

CLAAS. (2018). Technical data ATOS 350-220 (technical data sheet). Retrieved from https://www.claas.co.uk/blueprint/servlet/blob/1658072/cb561f5800d81eefcd2b4c1805b256f1/241563-23-dataRaw.pdf (HRC/336012130119 KK LC 0319). Retrieved 2019-08-15.

Daalgard, T., Halberg, N., & Porter, J. R. (2001). A model for fossil energy use in Danish agriculture used to compare organic and conventional farming. *Agriculture, Ecosystems & Environment, 87*, 51–65.

de Toro, A., & Hansson, P.-A. (2004). Analysis of field machinery performance based on daily soil workability status using discrete event simulation or on average workday probability. *Agricultural Systems, 79*(1), 109–129. https://doi.org/10.1016/S0308-521X(03)00073-8.

Engström, J., Gunnarsson, C., Baky, A., Sindhöj, E., Eksvärd, J., Orvendal, J., et al. (2015). *Increasing the effectiveness of agricultural logistics – a case-study project of evaluating potential effects of various strategies*. Retrieved from RISE, Uppsala, Sweden http://www.transportportal.se/Energieffektivitet/Etapp2/Energieffektivisering-av-jordbrukets.pdf.

Engström, J., & Lagnelöv, O. (2018). An autonomous electric powered tractor - simulations of all operations on a Swedish dairy farm. *Journal of Agricultural Science and Technology A, 8*(3), 182–187. https://doi.org/10.17265/2161-6256/2018.03.006.

Fendt. (2017). MARS: Robot system for planting and accurate documentation [Press release]. Retrieved from https://www.fendt.com/int/fendt-mars.html.

Green, O., Schmidt, T., Pietrzkowski, R., Jensen, K., Larsen, M., Edwards, G., et al. (2014). *Commercial autonomous agricultural platform - kongskilde Robotti. Paper presented at the second international Conference on robotics and associated high-technologies and equipment for agriculture and forestry, Madrid, Spain*. http://hdl.handle.net/10261/130548.

Grimstad, L., & From, P. J. (2017). Thorvald II - a modular and Re-configurable agricultural robot. *IFAC-PapersOnLine, 50*(1), 4588–4593. https://doi.org/10.1016/j.ifacol.2017.08.1005.

Grunditz, E., & Thiringer, T. (2016). Performance analysis of current BEVs based on a comprehensive review of specifications. *IEEE Transactions on Transportation Electrification, 2*(3), 270–289.

Hamidi, S. A., Ionel, D. M., & Nasiri, A. (2015). Modeling and management of batteries and ultracapacitors for renewable energy support in electric power systems–an overview. *Electric Power Components and Systems, 43*(12), 1434–1542. https://doi.org/10.1080/15325008.2015.1038757.

Harighi, T., Bayindir, R., & Hossain, E. (2018). Overviewing quality of electric vehicle charging stations' service evaluation. *International Journal of Smart Grid, 2*(1), 40–48. Retrieved from https://www.researchgate.net/publication/325286105_Overviewing_Quality_of_Electric_Vehicle_Charging_Stations.Service_Evaluation.

John Deere. (2017). *SIMA awards for innovation* [Press release]. Retrieved from https://www.deere.co.uk/en/our-company/news-and-media/press-releases/2017/feb/sima-awards-for-innovation.html.

Kim, J., Song, I., & Choi, W. (2015). An electric bus with a Battery exchange system. *Energies, 8*, 6806–6819. https://doi.org/10.3390/en8076806.

Kitani, A., Jungbluth, T., Peart, R. M., Ramdani, A., Badger, P. C., & Clark, N. R. (1999). CIGR handbook of agricultural engineering. In A. Kitani (Ed.), *Energy and biomass engineering): American society of agricultural engineers* (Vol. 5).

Klein, R., Chaturvedi, N. A., Christensen, J., Ahmed, J., Findeisen, R., & Kojic, A. (2011). *Optimal charging strategies in lithium-ion battery*. San Francisco, CA, USA: Paper presented at the American Control Conference.

Lincoln University. (2008). In T. Chaston (Ed.), *Financial budget manual 2008*. Lincon University, Lincoln, Canterbury, N.Z: Agriculture and Life Sciences Division. ISSN 113-1397.

Lindgren, M., Pettersson, O., Hansson, P.-A., & Norén, O. (2002). *Engine load pattern and engine exhaust gas emissions from off-road vehicles and methods to reduce fuel-consumption and engine exhaust gas emissions*. JTI, ISSN 1401-4963 (Retrieved from: http://www.diva-portal.org/smash/get/diva2:959556/FULLTEXT01.pdf (2019-08-15).

Lucas, A., Trentadue, G., Scholz, H., & Otura, M. (2018). Power quality performance of fast-charging under extreme temperature conditions. *Energie, 11*(10). https://doi.org/10.3390/en11102635.

Moreda, G. P., Muñoz-García, M. A., & Barreiro, P. (2016). High voltage electrification of tractor and agricultural machinery – a review. *Energy Conversion and Management, 115*, 117–131. https://doi.org/10.1016/j.enconman.2016.02.018.

Mueller, L., Lipiec, J., Kornecki, T. S., & Gebhardt, S. (2011). Trafficability and workability of soils. In J. Gliński, J. Horabik, & J. Lipiec (Eds.), *Encyclopedia of agrophysics* (pp. 913–924). Springer Publishing.

Myrbeck, Å. (1998). *Swedish Agricultural and Horticultural crops*. Solna, Sweden: Swedish Chemicals Agency, PM1/98.

Nilsson, B. (1976). *Planering av jordbrukets maskinsystem. Problem, modeller och tillämpningar*. Uppsala, Sweden: Swedish university of Agricultural Sciences. Report no 38. Department of Work Methodology and Technology.

Nilsson, D., & Bernesson, S. (2009). *Straw as fuel Part 2: Moisture characteristics*. Uppsala, Sweden: Swedish university of Agricultural Sciences. ISSN 1654-9406. https://pub.epsilon.slu.se/4852/1/nilsson_d_et_al_100630_2.pdf. (Accessed 18 September 2019).

Nilsson, D., & Bernesson, S. (2010). *Straw as fuel - Part 3: Dynamic simulation of handling systems*. Uppsala, Sweden: Swedish university of Agricultural Sciences. ISSN 1654-9406. https://pub.epsilon.slu.se/4815/1/nilsson_d_et_al_100629.pdf. (Accessed 18 September 2019).

Nilsson, D., & Hansson, P.-A. (2001). Influence of various machinery combinations, fuel proportions and storage capacities on costs for co-handling of straw and reed canary grass to district heating plants. *Biomass and Bioenergy, 20*(4), 247–260. https://doi.org/10.1016/S0961-9534(00)00077-5.

Nilsson, D., Larsolle, A., Nordh, N.-E., & Hansson, P.-A. (2017). Dynamic modelling of cut-and-store systems for year-round deliveries of short rotation coppice willow. *Biosystems Engineering, 159*(July 2017), 70–88. https://doi.org/10.1016/j.biosystemseng.2017.04.010.

Nilsson, D., Rosenqvist, H., & Bernesson, S. (2014). *Time demand for machine operations in small fields - a simulation study*. Uppsala, Sweden: Swedish university of Agricultural Sciences. ISSN 1654-9406. https://pub.epsilon.slu.se/11860/11/nilsson_et_al_150206%20.pdf. (Accessed 18 September 2019).

Oksanen, T. (2015). Accuracy and performance experiences of four wheel steered autonomous agricultural tractor in sowing operation. In L. Mejias, P. Corke, & J. Roberts (Eds.), *Field and service robotics* (Vol. 105, pp. 425–438). Berlin: Springer-Verlag Berlin.

Paulsson, R., Djodjic, F., Ross, C. C., & Hjerpe, K. (2015). *Nationell Jordartskartering*. Retrieved from https://www2.jordbruksverket.se/download/18.4288f19214fb7ec78849af18/1441973777932/ra15_19.pdf.

Reif, K., & Dietsche, K.-H. (2014). In K. Reif (Ed.), *Bosch automotive handbook* (9th ed.). Germany: John Wiley & Sons Ltd.

Ryu, I. H., Kim, D. C., & Kim, K. U. (2003). Power efficiency characterstics of a tractor drive train. *Transactions of the Asae, 46*(6), 1481–1486.

Safa, M., Samarasinghe, S., & Mohssen, M. (2010). Determination of fuel consumption and indirect factors affecting it in wheat production in Canterbury, New Zealand. *Energy, 35*, 5400–5405. https://doi.org/10.1016/j.energy.2010.07.015.

Serrano, J. M. P., José, O., da Silva, J. M., Pinheiro, A., & Carvalho, M. (2007). Tractor energy requirement in disc harrow systems. *Biosystems Engineering, 98*(3), 286–296. https://doi.org/10.1016/j.biosystemseng.2007.08.002.

Shen, W., Tu Vo, T., & Kapoor, A. (2012). *Charging algorithms of lithium-ion batteries: An overview. Paper presented at the 7th IEEE Conference on Industrial Electronics and Applications (ICIEA)*.

SMHI. (2019). *Meterological obesrvations: Precipitation* [Meterological data]. Enköing MO; Uppsala AUT Uppsala FLYGPLATS. Retrieved from: https://www.smhi.se/klimatdata/meteorologi/ladda-ner-meteorologiska-observationer#param=precipitationHourlySum,stations=all.

Song, J. K. I., & Choi, W. (2015). An electric bus with a Battery exchange system. *Energies, 8*, 6806–6819. https://doi.org/10.3390/en8076806.

Statistics Sweden. (2018). *Agricultural statistics 2018*. Retrieved from http://www.jordbruksverket.se/download/18.563019b71642b2ff18eee2a6/1530098111546/Kapitel%204%20Sk%C3%B6rdar.pdf.

Tan, X., Sun, B., Wu, Y., & Tsang, D. (2018). Asymptotic performance evaluation of battery swapping and charging station for electric vehicles. *Performance Evaluation, 119*, 43–57. https://doi.org/10.1016/j.peva.2017.12.004.

Tremblay, O., Dessaint, L.-A., & Dekkiche, A.-I. (2007). *A generic battery model for the dynamic simulation of hybrid electric vehicles.* Arlington, TX, USA: Paper presented at the IEEE Vehicle Power and Propulsion Conference.

Volpato, C. E. S., Paula, V. R.d., Barbosa, J. A., & Volpato, E. L. (2016). *Evaluation of the operational viability of the use of electricity as a source of power in agricultural tractors.* 2016 *ASABE Annual International Meeting, Orlando, Florida, USA, 17-20 July, 2016*, 162458121. Retrieved from <Go to ISI>://CABI:20173200350.

Wasilewski, J., Kuranc, A., Szyszlak-Bargłowicz, J., Stoma, M., Słowik, T., & Barta, D. (2017). *Assessment of efficiency of an agricultural tractor engine for different rotational speeds. Paper presented at the IX international scientific symposium: Farm machinery and processes management in sustainable agriculture, lublin, Poland*.

Wells, C. (2001). *Total energy indicators of agricultural sustainability: Dairy farming case study*. Wellington, NZ: Ministry of Agriculture and Forestry. Technical Paper 2001/3, ISSN: 1171-4662.

Witney, B. (1988). *Choosing and using farm machines*. London: Longman Scientific & Technical.

Yilmaz, M., & Krein, P. T. (2013). Review of battery charger topologies, charging power levels, and infrastructure for plug-in electric and hybrid vehicles. *IEEE Transactions on Power Electronics, 28*(5), 2151–2169. https://doi.org/10.1109/tpel.2012.2212917.

Young, S. N., Kayacan, E., & Peschel, J. M. (2018). Design and field evaluation of a ground robot for high-throughput phenotyping of energy sorghum. *Precision Agriculture*, 1–26. https://doi.org/10.1007/s11119-018-9601-6.